arXiv:cond-mat/0401023v1 [cond-mat.dis-nn] 3 Jan 2004

History-Induced Critical Behavior in Disordered Systems

John H. Carpenter, Karin A. Dahmen, Andrea C. Mills, and Michael B. Weissman
University of Illinois at Urbana-Champaign, Department of Physics, 1110 West Green Street, Urbana, IL 61801.

Andreas Berger and Olav Hellwig
Hitachi Global Storage Technologies, San Jose Research Center, 650 Harry Road, E3 San Jose, CA 95120.

(Dated: December 30, 2021)

Barkhausen noise as found in magnets is studied both with and without the presence of long-range (LR) demagnetizing fields using the non-equilibrium, zero-temperature random-field Ising model. Two distinct subloop behaviors arise and are shown to be in qualitative agreement with experiments on thin film magnets and soft ferromagnets. With LR fields present subloops resemble a self-organized critical system, while their absence results in subloops that reflect the critical point seen in the saturation loop as the system disorder is changed. In the former case, power law distributions of noise are found in subloops, while in the latter case history-induced critical scaling is studied in avalanche size distributions, spin-flip correlation functions, and finite-size scaling of the second moments of the size distributions. Results are presented for simulations of over 10^8 spins.

PACS numbers: 75.60.Ej, 75.70.Ak, 64.60.Ht, 75.60.Ch

Hysteresis occurs when a system far from equilibrium is driven by an external force. The system state then depends on the history of the system. In many systems such as ferromagnets [1], superconductors [2, 3], and martensites [4], the response to the driving force is not continuous but occurs in discrete jumps which is often referred to as "crackling noise", or specifically for magnets, Barkhausen noise. In magnets, broad ranges of power-law scaling of noise have been attributed to either a disorder induced critical point, such as found in the non-equilibrium zero temperature random-field Ising model (RFIM) [5], or to self-organized criticality (SOC) [6], as found in soft magnets.

The disorder induced critical point found in the saturation magnetization curve, traced out as an external magnetic field drives the system from one saturated state to the oppositely magnetized state and back, has been studied in detail for the RFIM [5, 7, 8, 9] and its existence has been experimentally confirmed [10]. However, taking magnets to saturation often is impractical due to the large magnetic fields required, so the behavior of subloops is of great interest to experiments and applications alike. The RFIM may be used to model subloops, and magnetization curves have been computed exactly in one dimension [11] and on a Bethe lattice [12] and have also been collapsed near the demagnetized state using Rayleigh's Law [13]. Also, the idea of history acting as a source of effective disorder was recently introduced [14]. In this letter we report how the presence or lack of long range (LR) demagnetizing fields produces two distinct behaviors in subloops of the RFIM. In particular, in the presence of sufficiently large LR fields, subloops are found to resemble a SOC system. However, in the absence of LR fields, we find a *critical subloop* inside the saturation loop where the system history acts as a tuning parameter instead of the system disorder. Correspondingly, a modified scaling picture for subloops, consistent with the saturation loop, is introduced. For both cases we report new experimental results for subloops showing qualitative agreement with the two behaviors of the RFIM.

In the non-equilibrium, zero-temperature RFIM spins $s_i = \pm 1$ are placed on a hyper-cubic lattice. At each site i a quenched random local field h_i is chosen from a Gaussian distribution, $\rho(h_i) = \frac{1}{\sqrt{2\pi}R} exp(-\frac{h_i^2}{2R^2})$. The field h_i acts as a source of disorder for the system, and the standard deviation R of the random distribution is termed the 'disorder'. The energy of a system with N spins is given by [15]

$$\mathcal{H} = -J\sum_{\langle ij\rangle} s_i s_j - \sum_i (h_i + H)s_i + \frac{J_{LR}}{N}\sum_{ij} s_i s_j, \quad (1)$$

where H is a tunable external magnetic field. The first term of Eq. 1 couples nearest-neighbor spins ferromagnetically ($\langle ij\rangle$ implies summing over nearest-neighbor pairs of spins) while the last term provides an infinite range anti-ferromagnetic (AF) coupling, where one sums over all pairs of spins regardless of their relative distance. This AF coupling models the dipolar interactions relevant in soft ferromagnets, which Zapperi, et. al. [6, 16] have shown in three dimensions to have the same effect on long length scales as infinite range mean field interactions. Note that by choosing $J_{LR} = 0$ one recovers the nearest-neighbor RFIM. In order to model hysteresis we study the model at zero temperature, far from thermal equilibrium [5, 8], and for convenience set $J = 1$.

Simulations of the above model were run by starting with the external field at $H = -\infty$ with all spins down, and then adiabatically slowly moving the external field through a particular history. As the field H is changed, a given spin will flip (either upwards or downwards) when its effective local field, $h_i^{eff} = H + h_i + J\sum_{\langle ij\rangle} s_j - J_{LR}M$,

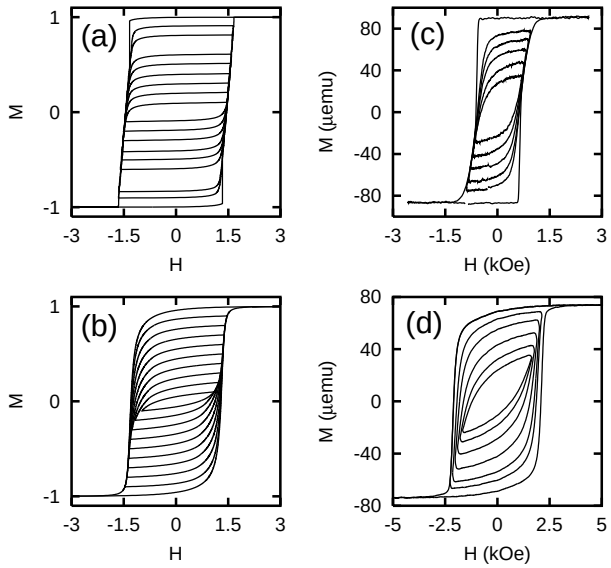


FIG. 1: Hysteresis loops with concentric inner subloops for (a) RFIM with 240^3 spins, $J_{LR} = 0.25$, and $R = 1.8$, (b) RFIM with 240^3 spins, $J_{LR} = 0$, and $R = 2.7$, (c) a Co/Pt multilayer thin film, and (d) a CoPtCrB alloy thin film.

changes sign. Here $M = \frac{1}{N}\sum_i s_i$ is the magnetization of a system with N spins. When a spin flips, it may induce its neighboring (or for $J_{LR} \neq 0$ even distant) spins to flip, creating an avalanche of flipping spins, which is the analog of a Barkhausen pulse. The simulations are based on the code available on the web [17] which has been modified to allow for subloops in the history. The code uses the sorted list algorithm, which stores the random fields, and is described in depth in Ref. [18].

In the absence of LR fields, as one tunes the system disorder (R), the RFIM exhibits a non-equilibrium second order phase transition at a critical disorder $R = R_c$ [5]. Below R_c the coupling of nearest-neighbors dominate the dynamics, and there is a finite jump in magnetization of the saturation loop. However, above R_c the random fields dominate, resulting in smooth hysteresis curves and mostly small avalanches. Many quantities associated with this critical point display scaling behavior for $R \to R_c$. A detailed discussion is given in Ref. [8].

The two distinct behaviors of subloops in the RFIM can be seen in Figure 1. In Fig. 1(a) subloops spaced by $\Delta M = 0.1$ are shown for a system with $J_{LR} = 0.25$ and a disorder of $R = 1.8$, chosen smaller than $R_c = 2.16$ as many experimental samples such as soft ferromagnets are believed to be below the critical disorder. The subloops show a linear $M(H)$ behavior as the field is increased, as one would expect for a system undergoing domain wall propagation while being exposed to a demagnetizing effect. Only the first few subloops show some effects of the initial condition (all spins down) before the sweeping field has created a large enough domain to allow for single domain wall propagation. On the other hand one finds a very different picture in the absence of LR fields. In Fig. 1(b), obtained for a system with $J_{LR} = 0$, $R = 2.7$ and subloop spacing $\Delta M = 0.1$, as one moves inwards, subloops begin to resemble the saturation loop at an effectively higher disorder, i.e. $R > 2.7$. Indeed, preflipped spins not participating in a given subloop may act as an added, possibly correlated, "effective disorder." Tuning the history in this way, we were unable to directly observe a transition from loops with a jump in magnetization to smooth inner subloops. This is due to the inability to break up the system spanning avalanche present below the critical disorder even for the largest simulated system sizes (480^3 spins) [13, 14, 19].

Experimental magnetization curves for thin films also exhibit these two types of behavior depending on the presence of LR fields. Fig. 1(c) displays magnetization curves for a Co/Pt-multilayer with the field applied along the surface normal. Due to the strong interface anisotropy of such multilayer samples, the easy axis of magnetization is perpendicular to the film plane even though the LR demagnetizing effect is largest in this direction. Despite the fairly rectangular major loop shape, indicating easy axis orientation, the loop exhibits an extended linear segment on which all minor loops merge due to the presence of LR dipolar effects. On the other hand, films with in-plane magnetization behave quite differently, because LR demagnetizing effects are extremely small in this geometry. Fig. 1(d) shows magnetization curves for a CoPtCrB-alloy film with the field applied in the film plane. This film is polycrystalline with grain sizes narrowly distributed around 10 nm diameter and exhibits strong exchange coupling between grains. Due to the lack of LR coupling, subsequent minor loops appear increasingly sheared with decreasing coercive field, very similar to the curves shown in Fig. 1(b) for the $J_{LR} = 0$ RFIM. All experimental data were measured at room temperature using an Alternating Gradient Magnetometer.

Much information on these two behaviors can be obtained by examining the Barkhausen noise present in the system. With LR fields present, the subloops display a power-law avalanche size distribution, all with the same exponent and cutoff size, indicating that the system is SOC [6, 15, 16]. Figure 2 displays the avalanche size distribution for subloops of a 21 cm x 1 cm x 30 μm ribbon of a $Fe_{21}Co_{64}B_{15}$ amorphous alloy. In the experiment, a solenoid provides a triangular driving field along the long axis of the sample at 0.03 Oe/s. The first cycle drives the sample to saturation, while subsequent cycles drive the field to successively smaller amplitudes (subloops). The driving rate is slow enough to ensure that avalanches do not overlap. The Barkhausen noise was measured with a pick-up coil of 150 turns of copper wire wound around the middle 0.3 cm of the sample. By integrating the pick-up voltage one may obtain the magnetization. The resulting hysteresis loops are shown

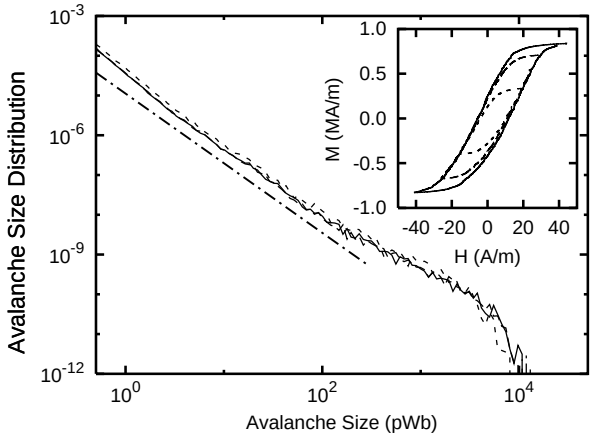


FIG. 2: Experimental avalanche size distributions for subloops of a soft ferromagnet. The three subloops analyzed are shown in the inset, with the largest corresponding to the saturation loop. The distributions were extracted from a window of width $\Delta H \approx 20A/m$ which started near $H = 0A/m$. A power law of -1.75 is show by the offset, dash-dot line.

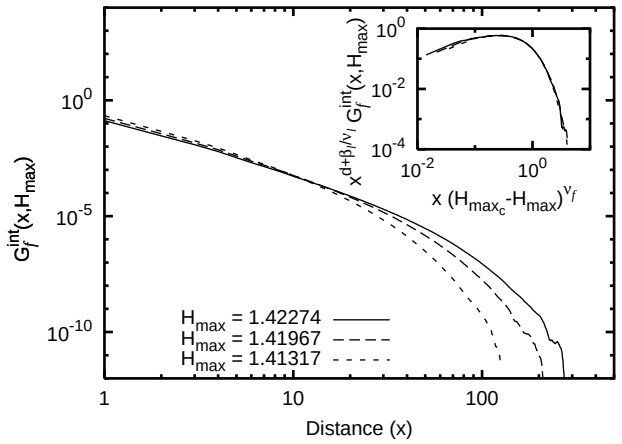


FIG. 3: Integrated spin-flip correlation functions for 480^3 systems at $R = 2.198$ and averaged over 20 random seeds. Curves are given for subloops starting at values of $H_{max} =$ 1.42274, 1.41967, and 1.41317. The inset contains a collapse of the three respective distributions, yielding $d+\beta_l/\nu_l = 3.0\pm0.2$ and $1/\nu_f = 1.28 \pm 0.40$ with $H_{max_c} = 1.427$.

in the inset of Fig. 2. The avalanche distributions for the subloops are all identical, affirming the SOC behavior. The measured power law exponent (1.75) is larger than has been predicted and measured for the saturation loop ($1.25 - 1.5$) [15, 16]. This is due to $M(H)$ not being strictly linear in the window analyzed. Choosing a smaller window close to the linear regime results in a power law exponent of 1.3, consistent with previous measurements. The RFIM with LR fields presents an almost identical picture of subloops. For a 240^3 system with $R = 1.8$ and $J_{LR} = 0.25$, subloops displayed identical power laws in their avalanche size distributions with a loop integrated exponent of 1.7 ± 0.2, in good agreement with the experimental results.

In the absence of LR fields the case is much different; the system history acts as a tuning parameter affecting a subloop dependent cutoff. Although a transition like the one found in the saturation loop cannot be directly observed, its existence may be ascertained by examining the scaling behavior on one side of ("above") the critical point [5, 8]. Thus we present a scaling collapse of loop integrated spin-flip correlation functions and a finite-size scaling collapse of the second moments of the integrated avalanche size distribution for subloops with $J_{LR} = 0$.

For the spin-flip correlation function, in analogy with the saturation loop [8] one may assume a scaling form

$$G^{int}(x, R, H_{max}) \sim x^{-(d+\beta_l/\nu_l)}\mathcal{G}^{int}(x(R - R_c^d)^{\nu_l}, xf^{\nu_f}), \quad (2)$$

where H_{max} is the maximum field along the subloop and $f = H_{max_c} - H_{max}$ is the history-induced analog of the reduced saturation loop disorder [21]. Here R_c^d is the critical disorder for the demagnetization curve which is numerically within the error bars of R_c. Similarly, $H_{max_c} = H_c^d$ is the critical field associated with the demagnetization curve [20]. According to scaling theory one expects the exponents $d + \beta_l/\nu_l$, ν_l, and ν_f as well as the scaling function $\mathcal{G}^{int}$ to be universal. Here a subscript l denotes an exponent associated with the random disorder scaling of the critical subloop and subscript f one associated with the history-induced "disorder". For the collapses, the system is run at the effective critical disorder of the saturation loop, $R_c(L)$, for the linear system size L with $R_c(L) \to R_c$ as $L \to \infty$. This system size dependent critical disorder $R_c(L)$ is defined as the disorder at which the maximum number of system spanning avalanches in the saturation loop is observed [8].

The integrated spin-flip correlation function, $G_f^{int}(x, H_{max})$, was measured for subloops spaced by $\Delta M_{max} = 0.025$ in their maximum magnetizations (see Fig. 3). A similar behavior to the saturation loop is found. As the history-induced disorder is increased, by moving to inner subloops, the curves display a decreasing cutoff. As the system is started at the effective critical disorder, Eq. 2 reduces to $G_f^{int}(x, H_{max}) \sim x^{-(d+\beta_l/\nu_l)}\mathcal{G}_f^{int}(xf^{\nu_f})$. This scaling ansatz results in the collapse shown in the inset of Fig. 3. Only subloops void of spanning avalanches were used in the collapses to remove the effects of the finite system size, equal to 480^3 spins.

The integrated avalanche size distribution, with a similar scaling ansatz $D_f^{int}(S, H_{max}) \sim S^{-(\tau+\sigma\beta\delta)_l}\mathcal{D}_f^{int}(S^{\sigma_f}f)$, was previously analyzed in Ref. [14]. The conclusions therein remain valid, and the exponents (see Table I) have been updated to correspond with the use of the scaling variable f.

Table I lists the exponents from the above two collapses along with the saturation loop values. While both power law behaviors, given by $\tau + \sigma\beta\delta$ and $d + \beta/\nu$, are

TABLE I: Universal critical exponents from scaling collapses in three dimensions for the history-induced disorder present in subloops and the random disorder of the saturation loop.

Exponent	History-Induced	Saturation[a]
$\tau + \sigma\beta\delta$	2.01 ± 0.10	2.03 ± 0.03
$1/\sigma$	2.3 ± 0.5	4.2 ± 0.3
$d + \beta/\nu$	3.0 ± 0.2	3.07 ± 0.30
$1/\nu$	1.28 ± 0.40	0.71 ± 0.09
ρ	2.6 ± 0.40	2.90 ± 0.16

[a]References [7, 8]

identical within error, the exponents governing the cutoff behavior, σ_f and ν_f, are found to differ from their saturation loop counterparts with only a slight overlap in their error estimates. One would expect identical values if the pre-flipped spins at the start of a subloop were randomly distributed about the lattice, thus preserving the uncorrelated, random nature of the system's disorder. However, this is not the case, as avalanches have left pockets of unflipped or preflipped spins of all sizes up to the system's correlation length. So the difference in exponents is not surprising as the history-induced disorder acts more like a correlated disorder as opposed to the uncorrelated, random system disorder R.

The second moments of the integrated avalanche size distribution also behave similarly to the saturation loop and have a scaling form, in analogy to the saturation loop and Eq. 2, $\langle S^2 \rangle_f^{int} \sim L^{-\rho_l} \mathcal{S}_f^2(fL^{1/\nu_f})$ where $\rho_l = -(\tau_l + \sigma_l\beta_l\delta_l - 3)/\sigma_l\nu_l$. Table I contains the exponents from a collapse for systems with sizes from $L = 80$ to $L = 480$. As each system size was run at the effective disorder, $R_c(L)$, a system size dependent $H_{max_c}(L)$ was required in the collapse. The exponent ν_f was chosen to be consistent across all collapses of the correlation function and second moments. Its value differs from the value of ν for the saturation loop, which reaffirms the differences between the history-induced and random disorder.

Two new exponents, σ_f and ν_f, were introduced to describe the history-induced scaling. However, only one is an independent exponent as they obey the exponent relation $\sigma_f\nu_f = \sigma_l\nu_l$, which may be derived from the relations in Ref. [20]. Additionally, the critical subloop exponents may be close to those of the saturation loop. Indeed, within error bars, numerical results have found equal power-law exponents. However, currently no exponent relations are known that require equality between the saturation loop and subloop (subscript l) exponents.

The RFIM has been used to investigate subloops of the main saturation hysteresis loop. Experimental measurement of subloops on thin film magnets both with and without LR forces showed qualitative agreement with the RFIM. In the presence of LR forces, subloops may be explained by simple domain wall propagation, as confirmed by Barkhausen noise measurements on soft magnets. However, in the absence of such forces the disordered critical point was reflected in subloops. Scaling collapses were performed for integrated avalanche size distributions, integrated correlation functions, and the second moments of the avalanche size distributions. Finally, it was shown that only one of the new critical exponents is independent of those found in the critical subloop.

We thank Jim Sethna and Gary Friedman for very useful discussions and Ferenc Pazmandi for suggesting to use H_{max} as the scaling variable instead of M_{max}. The work at UIUC was supported by NSF grant DMRs 99-76550 (MCC), 00-72783, and 02-40644, an A. P. Sloan fellowship (to K. D.), and an equipment award from IBM.

[1] P. J. Cote and L. V. Meisel, Phys. Rev. Lett. **67**, 1334 (1991).
[2] S. Field, J. Witt, and F. Nori, Phys. Rev. Lett. **74**, 1206 (1995).
[3] W. Wu and P. W. Adams, Phys. Rev. Lett. **74**, 610 (1995).
[4] E. Vives, J. Ortín, L. Mañosa, I. Ràfols, R. Pérez-Magrané, and A. Planes, Phys. Rev. Lett. **72**, 1694 (1994).
[5] J. P. Sethna, K. Dahmen, S. Kartha, J. A. Krumhansl, B. W. Roberts, and J. D. Shore, Phys. Rev. Lett. **70**, 3347 (1993).
[6] P. Cizeau, S. Zapperi, G. Durin, and H. E. Stanley, Phys. Rev. Lett. **79**, 4669 (1997).
[7] O. Perković, K. Dahmen, and J. P. Sethna, Phys. Rev. Lett. **75**, 4528 (1995).
[8] O. Perković, K. A. Dahmen, and J. P. Sethna, Phys. Rev. B **59**, 6106 (1999).
[9] K. Dahmen and J. P. Sethna, Phys. Rev. B **53**, 14872 (1996).
[10] A. Berger, A. Inomata, J. S. Jiang, J. E. Pearson, and S. D. Bader, Phys. Rev. Lett. **85**, 4176 (2000).
[11] P. Shukla, Phys. Rev. E **62**, 4725 (2000).
[12] P. Shukla, Phys. Rev. E **63**, 027102 (2001).
[13] L. Dante, G. Durin, A. Magni, and S. Zapperi, Phys. Rev. B **65**, 144441 (2002).
[14] J. H. Carpenter, K. A. Dahmen, J. P. Sethna, G. Friedman, S. Loverde, and A. Vanderveld, J. Appl. Phys. **89**, 6799 (2001).
[15] M. C. Kuntz and J. P. Sethna, Phys. Rev. B **62**, 11699 (2000).
[16] S. Zapperi, P. Cizeau, G. Durin, and H. E. Stanley, Phys. Rev. B **58**, 6353 (1998).
[17] M. C. Kuntz and J. P. Sethna, URL `http://www.lassp.cornell.edu/sethna/hysteresis/code`.
[18] M. C. Kuntz, O. Perković, K. A. Dahmen, B. W. Roberts, and J. P. Sethna, Comput. Sci. Eng. **1**, 73 (1999).
[19] M. C. Kuntz and J. P. Sethna, unpublished.
[20] J. H. Carpenter and K. A. Dahmen, Phys. Rev. B **67**, 020412(R) (2003).
[21] Ref. [14] used $\epsilon = (M_{max_c} - M_{max})/M_{max}$ for the history 'disorder'. However, f provides a sounder scaling picture.